

# State Feedback Speed Controller for Turbocharged Diesel Engine and Its Robustness

Dileep Malkhede and Bhartendu Seth

**Abstract**—In this paper, the full state feedback controllers capable of regulating and tracking the speed trajectory are presented. A fourth order nonlinear mean value model of a 448 kW turbocharged diesel engine published earlier is used for the purpose.

For designing controllers, the nonlinear model is linearized and represented in state-space form. Full state feedback controllers capable of meeting varying speed demands of drivers are presented. Main focus here is to investigate sensitivity of the controller to the perturbations in the parameters of the original nonlinear model. Suggested controller is shown to be highly insensitive to the parameter variations. This indicates that the controller is likely perform with same accuracy even after significant wear and tear of engine due to its use for years.

**Keywords**—Diesel engine model, Engine speed control, State feedback controller, Controller robustness.

## I. INTRODUCTION

**D**IESEL engines are used in most heavy duty applications. However, diesel engines suffer from some important drawbacks such as, low power density, lower engine operating speeds, rough running and smoke.

In addition to this, diesel engines have very serious shortcoming of instability without the proper controls [1]. One characteristic of diesel engine is that it has no natural top speed and tends to runaway under low load conditions. Under these conditions, the more the fuel is injected, since there is sufficient air for combustion, the faster the engine goes. The faster it goes, the faster the fuel gets injected. In such situation, the engine speed continues to increase until the engine literally flies apart. Diesel engines are traditionally equipped with a governor that limits the maximum speed of an engine by reducing the rate at which the fuel is injected. One of the important tasks for the diesel engine controller is to minimize the speed fluctuations. For large diesel applications, the issues of governing and control are therefore of critical importance.

With advances in electronics, control engineering, computers, sensors and actuators coupled with depleting world energy resources, it is highly desirable to develop new control strategies to improve the performance of existing engines in terms of robustness to load disturbance [2], [3], [4], [5], [6]. The main objectives of this paper are to use a detailed enough

Dr. Dileep Malkhede is working as a Professor in the Department of Mechanical Engineering, College of Engineering, Pune-05, India. (E-mail: dnm.mech@coep.ac.in) Phone: +919422918843.

Dr. Bhartendu Seth is an Ex-Professor of Mechanical Engineering Department, Indian Institute of Technology, Bombay-76, India. (E-mail: sethbarat@gmail.com).

nonlinear model of a turbocharged diesel engine and explore the state feedback controller and present that the controller is insensitive to parameter variations.

## II. NONLINEAR MODEL DEVELOPMENT

For designing an engine controller, a nonlinear engine model suitable for a control application is essential. Mean value engine modeling approach that describes dynamic engine variables (or states) as mean values rather than instantaneous values on time scales longer than an engine event is adopted.

A heavy-duty turbocharged 448 kW diesel engine is selected for the present study, which is used for marine and power generation applications. The schematic of the engine setup is shown in Fig. 1 and its specifications are given below.

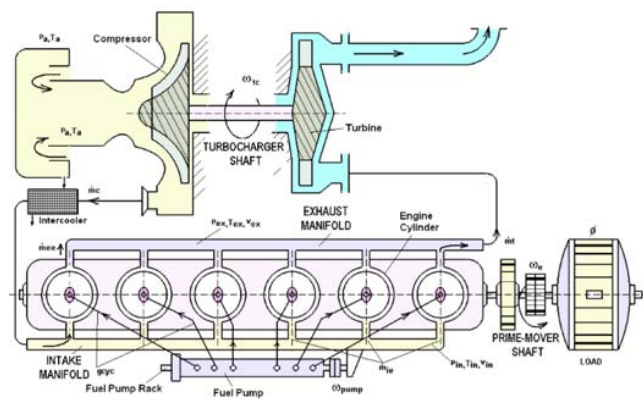


Fig. 1 Schematic of a TC Diesel Engine showing major subsystems

For obtaining the complete model, the engine was divided into four major subsystems. Each subsystem is then modeled individually. A set of differential equations of the four subsystems, viz., prime-mover (engine-load shaft), turbocharger, intake manifold and exhaust manifold of the engine were developed and may be studied in details from [2].

TABLE I  
ENGINE SPECIFICATIONS

Parameter	Description
Model	KTA-150 C-600
Make	Kirloskar Cummins
Turbocharger	T 18 A
H.P.	600
Rated speed	2100 rpm

No of cylinders	6
Bore	159 (mm)
Stroke	159 (mm)
Firing order	1-5-3-6-2-4

1. Prime-mover: The dynamics of the prime mover is characterized by a following first order nonlinear differential equation in engine shaft speed  $\omega_e$  based on Euler's law for rigid body rotation about fixed axis. Prime-mover dynamics assume a rigid crankshaft and constant average moment of inertia.

$$J_e \frac{d\omega_e}{dt} = M_e - M_t \quad (1)$$

The functional dependence of  $M_e$  and  $M_t$  are obtained as a function of input variables and other state variables of the system as expressed by Eq. (2) and (3) respectively.

$$M_e = f(h, \omega_e, p_{in}) \quad (2)$$

$$M_t = f(\omega_e, \phi) \quad (3)$$

2. Turbocharger: Turbine-compressor shaft dynamics is also modeled similar to that of the prime-mover equation.  $M_t$  and  $M_c$  are obtained as a function of other state variables and input variable as expressed by Eq. (4) and (5) respectively.

$$J_{tc} \frac{d\omega_{tc}}{dt} = M_t - M_c \quad (4)$$

$$M_t = f(\omega_{tc}, \omega_e, p_{ex}, p_{in}, h) \quad (5)$$

$$M_c = f(p_{in}, \omega_{tc}) \quad (6)$$

where,  $M_t$  and  $M_c$  are turbine and compressor torques ( $N.m$ ) and the moment of inertia of turbocharger rotor is denoted by  $J_{tc}$  in ( $kg.m^2$ ).

3. Intake Manifold: Intake manifold dynamics is modeled using the filling and emptying approach disregarding engine events and spatial variations of parameters within the manifold.

Mass flow rate  $\dot{m}_c$  is separately modeled using manufacturer supplied compressor characteristics and  $\dot{m}_{ie}$  is modeled using the engine pumping rate equation. The functional dependences are represented as,

$$\frac{dp_{in}}{dt} = \frac{RT_{in}}{v_{in}} (\dot{m}_c - \dot{m}_{ie}) \quad (7)$$

$$\dot{m}_c = f(p_{in}, \omega_{tc}) \quad (8)$$

$$\dot{m}_{ie} = f(p_{in}, \omega_e) \quad (9)$$

4. Exhaust Manifold: The rate of change of mass in exhaust manifold is modeled using the difference between the mass that enters the exhaust manifold from engine  $\dot{m}_{ee}$  and the mass  $\dot{m}_t$  that leaves the exhaust manifold and enters the turbine.

$$\frac{dm_{ex}}{dt} = \dot{m}_{ee} - \dot{m}_t \quad (10)$$

The compression or expansion of the gas in the exhaust manifold is assumed to be a polytropic process. Mass flow rate through the engine to the exhaust manifold  $\dot{m}_{ee}$  is considered as sum of air and fuel flow rates and  $\dot{m}_t$  is modeled using turbine characteristic map.

$$\dot{m}_{ee} = f(p_{in}, \omega_e, h) \quad (11)$$

$$\dot{m}_t = f(p_{ex}, h, \omega_{tc}, \omega_e, p_{in}) \quad (12)$$

The overall nonlinear model of their TC Diesel Engine is represented by a system of four coupled nonlinear differential equations viz., Eq. (1, 4, 7 and 10).

### III. LINEARIZATION OF THE NONLINEAR MODEL

Linearization is carried out at an operating point where the engine torque and speed are 1770  $N.m$  and 220  $rad/s$  (or 2100  $rpm$ ), respectively. At this operating point, the engine is at about 85 % of its rated load. Diesel engines normally run close to this loading condition and thus ideally suited for controller design.

1. Prime-mover:

$$\tau_e \frac{d\hat{\omega}}{dt} + k_e \hat{\omega}_e = \hat{h} + a_e \hat{p}_{in} - b_e \hat{\phi} \quad (13)$$

Where, coefficients of the equation are given by,

$$\tau_e = J_e \left( \frac{\partial M_e}{\partial h} \right)^{-1} \left( \frac{\omega_{eo}}{h_o} \right)$$

$$k_e = F_e \left( \frac{\partial M_e}{\partial h} \right)^{-1} \left( \frac{\omega_{eo}}{h_o} \right)$$

$$F_e = \left( \frac{\partial M_t}{\partial \omega_e} \right) - \left( \frac{\partial M_e}{\partial \omega_e} \right)$$

$$a_e = \left( \frac{\partial M_e}{\partial p_{in}} \right) \left( \frac{\partial M_e}{\partial h} \right)^{-1} \left( \frac{p_{in,o}}{h_o} \right)$$

$$b_e = \left( \frac{\partial M_t}{\partial \phi} \right) \left( \frac{\partial M_e}{\partial h} \right)^{-1} \left( \frac{\phi_o}{h_o} \right)$$

Similarly, other three nonlinear equations are linearized, the Equations are given below.

2. Turbocharger:

$$\tau_{tc} \frac{d\hat{\omega}_{tc}}{dt} + k_{tc} \hat{\omega}_{tc} = \hat{p}_{ex} + a_{tc} \hat{\omega}_e + b_{tc} \hat{p}_{in} + c_{tc} \hat{h} \quad (14)$$

3. Inlet Manifold:

$$\tau_{in} \frac{d\hat{p}_{in}}{dt} + k_{in} \hat{p}_{in} = \hat{\omega}_{tc} - a_{in} \hat{\omega}_e \quad (15)$$

4. Exhaust Manifold:

$$\tau_{ex} \frac{d\hat{p}_{ex}}{dt} + k_{ex} p_{ex} = \hat{\omega}_e + a_{ex} \hat{p}_{in} + b_{ex} \hat{h} - c_{ex} \hat{\omega}_{tc} \quad (16)$$

Above four differential equations are linearized equations of the model. Normalized variables of the linearized equations are given below. These equations relate normalized variables with physical engine variables.

$$\begin{aligned} \hat{\omega}_e &= \frac{\Delta \omega_e}{\omega_{e_o}}; & \hat{\omega}_{tc} &= \frac{\Delta \omega_{tc}}{\omega_{tc_o}}; & \hat{p}_{in} &= \frac{\Delta p_{in}}{p_{in_o}} \\ \hat{p}_{ex} &= \frac{\Delta p_{ex}}{p_{ex_o}}; & \hat{h} &= \frac{\Delta h}{h_o}; & \hat{\phi} &= \frac{\Delta \phi}{\phi_o} \end{aligned}$$

The overall model obtained after coupling all the above equations has two inputs, viz.,

(i) A normalized fuel rack position  $\hat{h}$  which acts as the controlling input and,

(ii) A propeller pitch  $\hat{\phi}$ , which is related to external load and acts as a disturbance.

Overall model gives four normalized state-variables viz.,  $\hat{\omega}_e$ ,  $\hat{\omega}_{tc}$ ,  $\hat{p}_{in}$  and  $\hat{p}_{ex}$ . As the study is focussed on speed control of the engine  $\hat{\omega}_e$ , is of prime importance.

Set of linearized equations are presented in state-space form as given below.

$$\dot{\hat{x}} = A\hat{x} + B\hat{u} \quad (17 a)$$

$$\hat{y} = C\hat{x} + D\hat{u} \quad (17 b)$$

Open loop responses of the linearized model are compared with that of the nonlinear model to verify the suitability of the linearized models for control systems designs. One such comparison is presented in Fig. 2. while  $h$  is perturbed by +10% and  $\phi$  maintained at  $\phi_o$ . It can be seen that, the dynamics is captured by linearized model and its response match well with that of the nonlinear system.

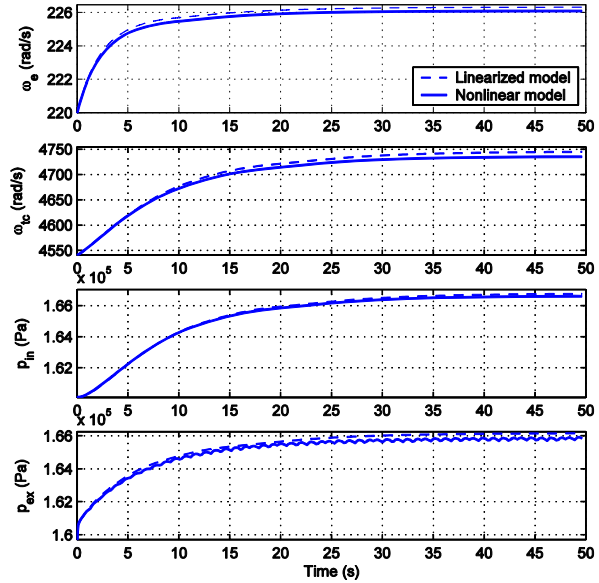


Fig. 2 Comparison of responses of linearized and nonlinear model

#### IV. STATE FEEDBACK DESIGN FOR SPEED TRACKING

A system is represented in state-space by the following equations.

$$\dot{\hat{x}} = A\hat{x} + B\hat{u} \quad (18 a)$$

$$\hat{y} = C\hat{x} + D\hat{u} \quad (18 b)$$

Where,

$\hat{x}$  is normalized state vector.

$\hat{y}$  is normalized output.

$\hat{u}$  is normalized input.

**Controllability of the system:** If the system is completely state controllable, then closed loop poles may be placed at any desired locations by means of state feedback through an appropriate state-feedback gain matrix  $K$ .

System matrices are,

$$A = \begin{bmatrix} -0.4555 & 0.0 & 0.0438 & 0.0 \\ 0.0058 & -0.3285 & 0.0437 & 0.2875 \\ -2.1564 & 10.4769 & -9.9054 & 0.0 \\ 6.0408 & 2.3730 & 3.1573 & -12.0195 \end{bmatrix}$$

$$B = \begin{bmatrix} 0.1109 \\ 0.0131 \\ 0.0 \\ 0.7157 \end{bmatrix} \quad \text{and} \quad C = [1 \quad 0 \quad 0 \quad 0]$$

The controllability matrix  $M$  is given by

$$M = [B \quad AB \quad A^2B \quad A^3B]$$

The matrix  $M$  is of full rank, hence the system is completely state controllable and arbitrary pole placement is possible.

This section presents the state feedback design with an integrator that is capable of tracking the desired speed. Now that the integrator is added, the order of the model is increased to 5. The plant has no zero at the origin and thus the possibility of cancellation of added integrator is avoided. The complete block diagram is shown in Fig. 3.

Following are the system state-space equations.

$$\dot{\hat{x}} = A\hat{x} + B\hat{u} \quad (19 \text{ a})$$

$$\hat{y} = C\hat{x} \quad (19 \text{ b})$$

$$\dot{\hat{u}} = -K\hat{x} + K_I\hat{\xi} \quad (20)$$

$$\dot{\hat{\xi}} = \hat{r} - \hat{y} \quad (21 \text{ a})$$

$$= \hat{r} - C\hat{x} \quad (21 \text{ b})$$

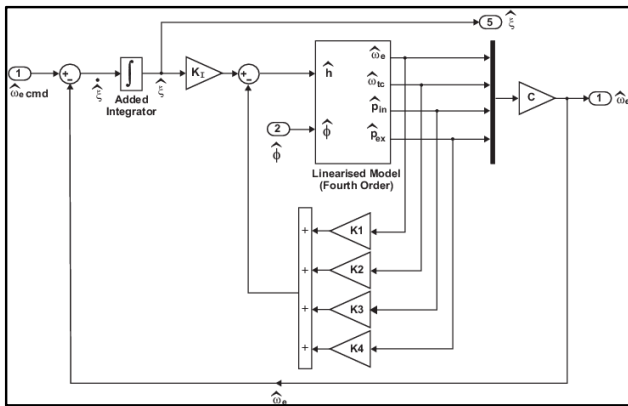


Fig. 3 Block diagram of state feedback with an integrator

$\hat{x}$  is a normalized state vector of the fourth order plant.

$\hat{u}$  is a normalized controlling input.

$\hat{y} = \hat{\omega}_e$  is a normalized engine speed (output signal)

$\hat{\xi}$  is the output of an integrator, added state of the system.

$\hat{r}$  is reference input signal, a state function.

Reference step input is applied at  $t = 0$ . Then the system dynamics is described by an equation that is a combination of dynamical Eqs. (19 a) and (21 a).

$$\begin{bmatrix} \dot{\hat{x}}(t) \\ \dot{\hat{\xi}}(t) \end{bmatrix} = \begin{bmatrix} A & 0 \\ -C & 0 \end{bmatrix} \begin{bmatrix} \hat{x}(t) \\ \hat{\xi}(t) \end{bmatrix} + \begin{bmatrix} B \\ 0 \end{bmatrix} \hat{u}(t) + \begin{bmatrix} 0 \\ 1 \end{bmatrix} \hat{r}(t) \quad (22)$$

The system is designed such that  $\hat{x}(\infty)$ ,  $\hat{\xi}(\infty)$  and  $\hat{u}(\infty)$  approaches constant values. Then, at steady-state,  $\dot{\hat{\xi}}(\infty) = 0$  and we get  $\hat{y}(\infty) = \hat{r}$ .

At steady-state, we have,

$$\begin{bmatrix} \hat{x}(\infty) \\ \hat{\xi}(\infty) \end{bmatrix} = \begin{bmatrix} A & 0 \\ -C & 0 \end{bmatrix} \begin{bmatrix} \hat{x}(\infty) \\ \hat{\xi}(\infty) \end{bmatrix} + \begin{bmatrix} B \\ 0 \end{bmatrix} \hat{u}(\infty) + \begin{bmatrix} 0 \\ 1 \end{bmatrix} \hat{r}(\infty) \quad (23)$$

Since,  $r(t)$  is a reference step input we have,  $\hat{r}(\infty) = \hat{r}(t)$ , for  $t > 0$ . By subtracting (23) from Eq. (22),

$$\begin{bmatrix} \hat{x}(t) - \hat{x}(\infty) \\ \hat{\xi}(t) - \hat{\xi}(\infty) \end{bmatrix} = \begin{bmatrix} A & 0 \\ -C & 0 \end{bmatrix} \begin{bmatrix} \hat{x}(t) - \hat{x}(\infty) \\ \hat{\xi}(t) - \hat{\xi}(\infty) \end{bmatrix} + \begin{bmatrix} B \\ 0 \end{bmatrix} [\hat{u}(t) - \hat{u}(\infty)] \quad (24)$$

Defining,

$$\hat{x}(t) - \hat{x}(\infty) = \hat{x}_e(t) \quad (25)$$

$$\hat{\xi}(t) - \hat{\xi}(\infty) = \hat{\xi}_e(t) \quad (26)$$

$$\hat{u}(t) - \hat{u}(\infty) = \hat{u}_e(t) \quad (27)$$

Then, Eq. (24) can be written as,

$$\begin{bmatrix} \dot{\hat{x}}_e(t) \\ \dot{\hat{\xi}}_e(t) \end{bmatrix} = \begin{bmatrix} A & 0 \\ -C & 0 \end{bmatrix} \begin{bmatrix} \hat{x}_e(t) \\ \hat{\xi}_e(t) \end{bmatrix} + \begin{bmatrix} B \\ 0 \end{bmatrix} \hat{u}_e(t) \quad (28)$$

Where,

$$\hat{u}_e(t) = -K\hat{x}_e(t) + K_I\hat{\xi}_e(t) \quad (29)$$

Defining a new fifth order error vector  $e(t)$  by

$$\hat{e}(t) = \begin{bmatrix} \hat{x}_e(t) \\ \hat{\xi}_e(t) \end{bmatrix} \quad (30)$$

Equation (28) becomes,

$$\dot{\hat{e}} = \hat{A}\hat{e} + \hat{B}\hat{u}_e \quad (31)$$

Where,

$$\hat{A} = \begin{bmatrix} A & 0 \\ -C & 0 \end{bmatrix} \quad \text{and} \quad \hat{B} = \begin{bmatrix} B \\ 0 \end{bmatrix}$$

Equation (29) becomes,

$$\hat{u}_e = -\hat{K}\hat{e} \quad (32)$$

Where,

$$\hat{K} = [K \quad \dots \quad -K_I] \quad (33)$$

The state error equation can be obtained by substituting

Eq. (43) into Eq. (42).

$$\dot{\hat{e}} = (\hat{A} - \hat{B}\hat{K})\hat{e} \quad (34)$$

If the desired eigenvalues of matrix  $\hat{A} - \hat{B}\hat{K}$  are specified as  $\mu_1, \mu_2, \dots, \mu_{n+1}$ , then the state feedback gain matrix  $K$  and the integral gain constant  $K_I$  can be determined by pole placement technique for completely state controllable system.

If the matrix  $P = \begin{bmatrix} A & B \\ -C & 0 \end{bmatrix}$  has a rank equal to the order of new system i.e. if the rank of matrix  $P$  is 5, hence the system is thus completely state controllable [7]. The state error equation.

$$\dot{\hat{e}} = \hat{A}\hat{e} + \hat{B}\hat{u}_e \quad (35)$$

Control signal is given by an Eq. (32) and  $\hat{K}$  by Eq. (33). Closed loop poles of the original fourth order system are placed as,

$$\begin{aligned} \mu_1 &= -10 + 4i; & \mu_2 &= -10 - 4i; \\ \mu_3 &= -7 + 5i; & \mu_4 &= -7 - 5i \end{aligned}$$

Position of the fifth pole is however adjusted at  $\mu_5 = -0.1548$  to achieve zero steady-state error in minimum time. State feedback gain matrix for a fifth order system is obtained using pole placement. The state feedback gain matrix obtained is,

$$\begin{aligned} K &= [K_1 \quad K_2 \quad K_3 \quad K_4] \\ &= [103.49 \quad 32.64 \quad -30.02 \quad -0.64] \text{ and} \\ K_5 &= -K_I = 635.89 \end{aligned}$$

Closed loop speed responses are plotted with a command signal that comprises typical steps as shown in Fig. 4 (upper). The controller is evaluated then on linear model to ensure its suitability for the real system. Settling time for engine speed is observed to be 0.41 s with the linear and 0.85 s with the nonlinear model. Negligibly small overshoot of 2 % with linearized and 9.2 % with nonlinear model are observed. Results show that the responses of the states with linearized and nonlinear plant are in agreement. Fuel rack position is also plotted for both linearized and nonlinear plant. Due to augmentation of the integrator speed tracking is possible and steady-state error reduced to zero.

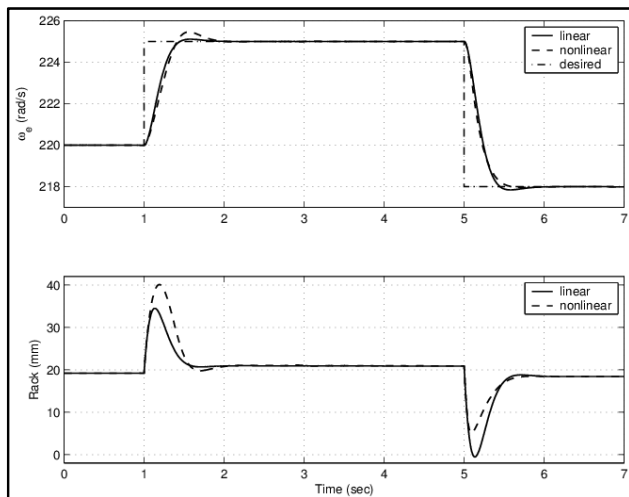


Fig. 4 Speed responses of state feedback with an integrator that utilizes full range of rack actuation

#### V. SENSITIVITY OF CLOSED LOOP PERFORMANCE TO PERTURBATIONS IN MODEL PARAMETERS

All control problems, encounter discrepancies between the actual plant dynamics and the dynamics of the model used for

controller design. The mismatch may appear due to unmodelled dynamics, variation in system parameters, linearization of the nonlinear model about an equilibrium point or the approximation of complex plant behaviour by a simpler model to ease the modelling and controller design processes.

It is also a fact that, closed loop systems are inherently robust against model uncertainties in contrast to the systems in open loop. Controllers that are not sufficiently robust can poorly perform or may lead to system instability. Therefore, in this part of the paper, sensitivity of the closed loop performance to the perturbations in the parameters of the original nonlinear model is investigated.

The nonlinear model developed in [2] includes variables such as indicated thermal efficiency  $\eta_i$ , volumetric efficiency  $\eta_v$ , friction mean effective pressure  $f_{mep}$  and temperature rise across the engine  $\Delta T_e$ . As applicable to any mathematical model, the dynamics of this model also may deviate from the physical engine, as a result of which the closed loop performance is likely to vary. It is therefore imperative to investigate the closed loop performance when the model is subjected to parameter variations. In this part, above four model parameters are varied one at a time by +10% and -10% from the nominal values and the closed loop performance of the tracking controller with such perturbed models is investigated.

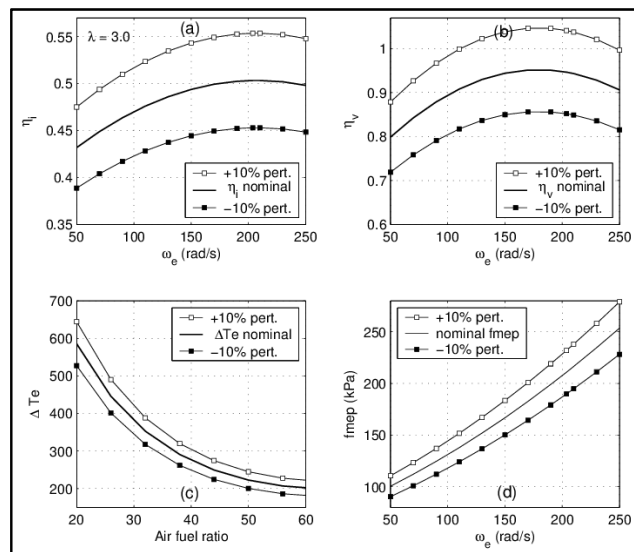
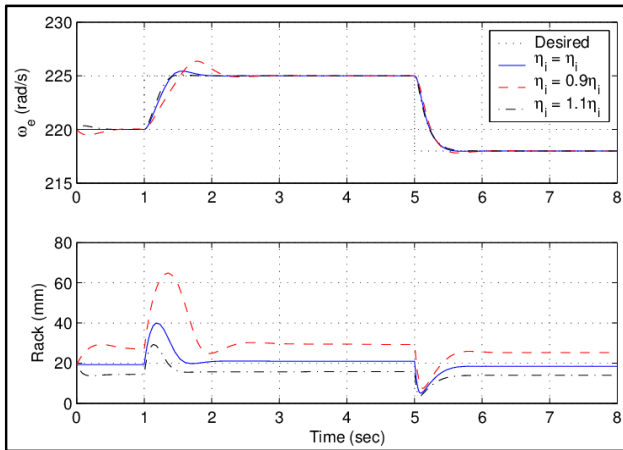


Fig. 5 Perturbations in  $\eta_i$ ,  $\eta_v$ ,  $\Delta T_e$  and  $f_{mep}$  from their nominal estimations considered for sensitivity analysis

Fig. 5 (a) through 5 (d) indicate the range of perturbations in the model parameters,  $\eta_i$ ,  $\eta_v$ ,  $\Delta T_e$  and  $f_{mep}$  respectively, from their nominal values due to +10% variation. Fig. 6, 7, 8 and 9 show the corresponding closed loop response of the system for the perturbations in  $\eta_i$ ,  $\eta_v$ ,  $\Delta T_e$  and  $f_{mep}$ .


 Fig.6 Sensitivity of performance to +10% perturbations in  $\eta_i$ .

When the nonlinear model is used without any perturbation in parameters, i.e. using their nominal values, the overshoot and the settling time are found to be 9.2% and 0.85 s respectively. Table II presents the performance parameters of the closed loop system with the perturbed models. Although the performance with perturbed models deviate compared to the ones with the nominal model but does not necessarily deteriorate. Positive perturbation in  $\eta_i$  and  $\eta_v$  both, have favourable effects on the performance since the overshoot and the settling time are reduced, and the vice-versa. Variation in  $\eta_i$  by +10% from its nominal value reduces the overshoot and the settling time to 2% and 0.7 s respectively. However, -10% perturbations in  $\eta_i$  is found to have increased the settling time and overshoot both. For +10% perturbation in  $\eta_v$ , the overshoot is reduced to 4.82 %, as also the settling time to 0.81 s.

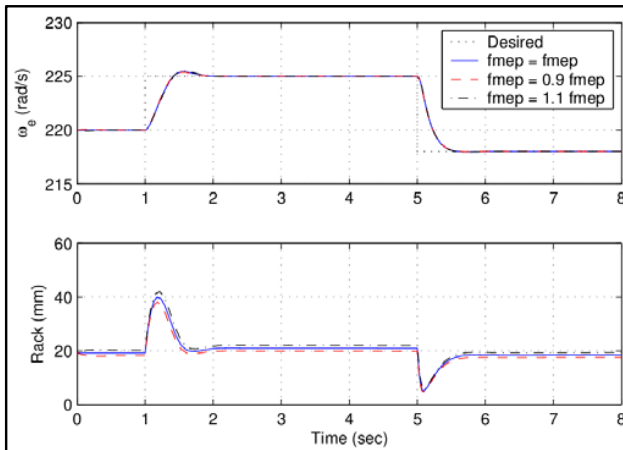
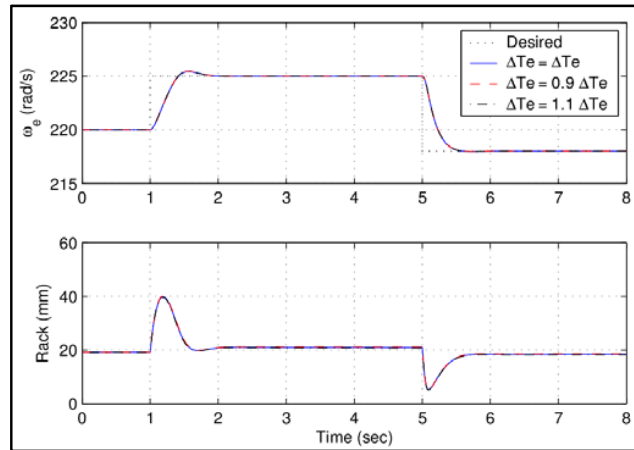
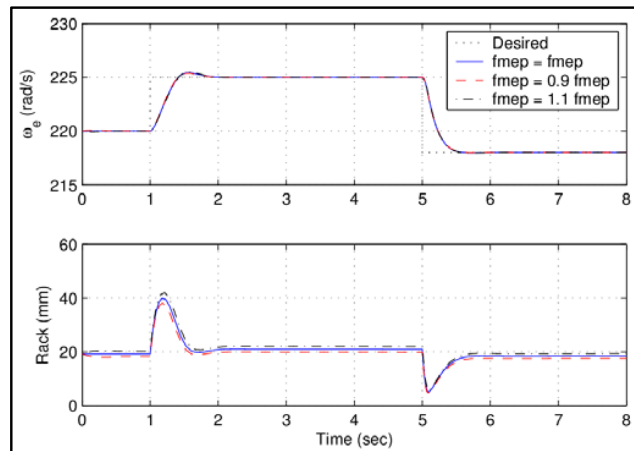

 Fig. 7 Sensitivity of performance to  $\pm 10\%$  perturbations in  $\eta_v$ .

 Fig. 8 Sensitivity of performance to  $\pm 10\%$  perturbations in  $\Delta T_e$ 

 Fig. 9 Sensitivity of performance to  $\pm 10\%$  perturbations in  $f_{\eta ep}$ 

 TABLE II  
EFFECT OF PERTURBATIONS IN PARAMETERS OF THE ENGINE MODEL

Model Parameters	+10%		-10%	
	$M_p$ (%)	$T_s$ (s)	$M_p$ (%)	$T_s$ (s)
$\eta_i$	2.0%	0.70	27.5%	1.22
$\eta_v$	4.82%	0.81	14.4%	1.02
$\Delta T_e$	0.92%	0.85	9.3%	0.85
$f_{\eta ep}$	10.8%	0.88	7.4%	0.83

Reduction in  $\eta_v$  by 10% has the reverse effect with overshoot and settling time increased to 14.4% and 1.02 s. The perturbations in  $\Delta T_e$  and  $f_{\eta ep}$  have the negligible effects on the performance. It may be noted from Fig. 8 and 9 that, inspite of a significantly large variation of  $\pm 10\%$  variations in the parameters, the closed loop system remains stable and the objectives of speed regulation continue to be met.

## VI. CONCLUSIONS

In this paper, the state-space model of the engine was augmented with an integrator for designing controller. with this design, speed tracking is achieved and steady-state error is reduced to zero. It is also observed that if the system parameters such as thermal efficiency, frictional losses,

volumetric efficiency and exhaust gas temperature are varied by as much as  $\pm 10\%$ , the closed loop response of the system is insensitive to such variation. This indicates that even if the controller is designed for new engine, it works even after several years of its use, indicating its robustness over the entire life of the engine.

## ABBREVIATIONS

$B$	Input matrix
$C$	Output matrix
$R$	Gas constant for air ( $J/kg.K$ )
$c_p$	Specific heat ( $J/kg.K$ )
$M$	Torque (N.m)
$J$	Reduced moment of inertia ( $kg.m^2$ )
$K$	State feedback gain matrix
$\phi$	Propeller pitch (Load) setting
$h$	Fuel rack position ( $mm$ )
$n_{ex}$	Polytropic constant of exhaust gas.
$\hat{x}$	Normalized form of state vector
$\hat{y}$	Normalized form of output
$\hat{\phi}$	Normalized variable for propeller pitch
$\dot{m}_{ie}$	Mass flow rate of air from intake manifold to the engine (kg/s)
$\dot{m}_{ee}$	Mass flow rate of exhaust from engine to exhaust manifold (kg/s)
$\dot{m}_c$	Mass flow rate through compressor (kg/s)
$\dot{m}_t$	Mass flow rate through turbine (kg/s)
$m_{in}$	Mass of air in intake manifold (kg)
$m_{ex}$	Mass of exhaust gas in the exhaust manifold (kg)

## SUBSCRIPTS

$a$	Ambient condition/an actual parameter
$c$	Compressor
$e$	Engine
$ex$	Exhaust manifold
$in$	Inlet manifold
$ie$	Inlet manifold to engine
$ee$	Engine to exhaust manifold
$T$	Turbine
$tc$	Turbocharger
$o$	Steady state values

## REFERENCES

- [1] Krutov V.I. "Automotive Control of Internal Combustion Engines", Mir Publishers, Moscow, 1987.
- [2] D. N. Malkhede, B. Seth and H.C. Dhariwal, "Mean Value Model and Control of a Marine Turbocharged Diesel Engine," SAE Technical Paper No. 2005-01-3889, 2005.
- [3] Guzzella L. and Amstutz A., Control of Diesel Engines, IEEE Control Systems Magazine, Vol. 8, No. 9, pp. 55-71, 1998.
- [4] Christen Urs, Vantine Katie and Collings Nick, Event-based Mean-Value Modelling of DI Diesel Engines for Controller Design, SAE Paper No. 2001-01-1242, 2001.
- [5] J. J. Moskwa and J.K. Hedrick, "Automotive Engine Modeling for Real Time Control Application," in Proc. of the 1987, IEEE American Control Conf., pp. 341-346, 1987.
- [6] M. Kao and J.J. Moskwa, "Nonlinear Diesel Engine Control and Cylinder Pressure Observation," Journal of Dynamic Systems, Measurement and Control, Vol. 117, Pages 183-192, June, 1995.
- [7] K. Ogata, Modern Control Engineering, Prentice Hall of India, 4th edition, 2002.